

# **Integrated Optical Circulator based on Radiatively Coupled Magneto optic Waveguides**

*M. Lohmeyer, M. Shamonin, P. Hertel*

*Department of Physics, University of Osnabrück,  
Barbarastraße 7, D-49069 Osnabrück, Germany*

**Abstract:** In a three-guide coupler with multimode central waveguide more than two modes of the entire structure participate in the coupling between the outer waveguides. Using a three mode approximation we found simple conditions for complete power transfer between the outer waveguides: the device length has to match certain multiples of the conventionally defined coupling length. The specific form of the relevant modes allows to design a magneto optic isolator or circulator with significantly reduced device length (as compared to the conventional nonreciprocal coupler). The performance of the proposed devices is simulated by propagating mode calculations. Estimates for admissible fabrication tolerances for the layer thicknesses are presented.

**Keywords:** integrated optics, radiatively coupled waveguides, three-guide coupler, magneto optic isolator, magneto optic circulator



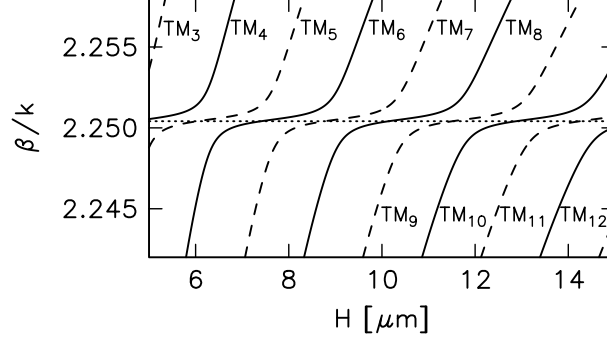


Figure 2: Effective mode indices for TM-polarized modes versus the thickness of the central layer. Remaining parameters are:  $\lambda = 1.3\mu\text{m}$ ,  $n_0 = n_2 = 2.18$ ,  $n_1 = n_3 = 2.30$ ,  $h = 0.8\mu\text{m}$ ,  $t = 0.8\mu\text{m}$ . Only a small fraction of the region allowed for the mode indices is displayed. Symmetric modes are indicated by continuous lines, antisymmetric modes by dashed lines. The dotted line shows the level  $\beta^*/k = 2.25041$ .

the central layer the mode function varies sinusoidally along the  $x$  coordinate with a spatial period of  $2\pi/\sqrt{k^2 n_3^2 - \beta^2}$ . Therefore, modes with the same propagation constant  $\beta$  exist in a set of waveguides with thicknesses  $H_j = H_0 + j\pi/\sqrt{k^2 n_3^2 - \beta^2}$  ( $j = 1, 2, \dots$ ), too. These modes are symmetric (even  $j$ ) or antisymmetric (odd  $j$ ) with respect to the reflection  $x \rightarrow -x$ . The shape of the mode function remains unchanged apart from the sine or cosine term inserted at  $H_j - H_0$ .

For each thickness  $H$  there are either two or three propagation constants close to  $\beta_*$ . The corresponding modes contribute with large amplitudes to light propagation if the structure is excited by the guided mode of one outer waveguide. In some cases the coupling behaviour may be well characterized by the interference of only three modes. Fig. 3 shows the corresponding mode functions and their superposition.

Let us now discuss the coupling of power between the two outer waveguides. Denote by  $\chi_j$  the normalized (guided) mode functions of the entire structure:  $\langle \chi_k, \chi_j \rangle = \delta_{kj}$ .  $\beta_j$  are the corresponding propagation constants. The scalar product for TM modes is  $\langle \phi, \chi \rangle = \int n(x)^{-2} \phi^*(x) \chi(x) dx$ , the inverse permittivity being absent for TE modes. For sufficiently large gap width  $t$  (cf. Fig. 1) this scalar product may serve to express the orthonormalization of the mode functions  $\phi_1, \phi_2$  of the outer waveguides WG1 and WG2 as well:  $\langle \phi_k, \phi_j \rangle = \delta_{kj}$ . Suppose the TM polarized mode  $\phi_1$  of waveguide WG1 with amplitude  $a_0$  is launched into the coupling region at  $z = 0$ . Reflections at the input will be neglected. The power transmitted to waveguide  $k = 1, 2$  at the end  $z = L$  of the coupling region is given by

$$P_k(L) = \left| \sum_j w_{kj} \exp(-i\beta_j L) \right|^2 \quad \text{with} \quad w_{kj} = \langle \phi_k, \chi_j \rangle \langle \chi_j, \phi_1 \rangle, \quad (1)$$

normalized to an input power  $\beta_* |a_0|^2 / (2\omega\epsilon_0) = 1$ . Reflections at output are again neglected.  $P_1$  denotes the power transfer to the input waveguide (A  $\rightarrow$  B in Fig. 1).

It is a very good approximation to restrict, in (1), the sum over *all* modes to *guided* modes of the entire structure. All devices studied in this paper show only low radiation losses at input and output,  $P_1(0) \geq 0.999$ . We therefore prefer to calculate the propagation of fields by representing them as superpositions of guided modes.

The weights  $c_j$  allow to classify the three mode approximation mentioned above. Consider the three modes  $\chi_-, \chi_0, \chi_+$  with increasingly ordered propagation constants  $\beta_-, \beta_0, \beta_+$  closest to  $\beta_*$ . Their contribution to the total power transmission is

$$\mathcal{P}_k(L) = \left| \sum_{j=-,0,+} w_{kj} \exp(-i\beta_j L) \right|^2. \quad (2)$$

For the structures discussed here,  $\mathcal{P}_1(0)$  turns out to be always larger than 0.9 (see Fig. 4).

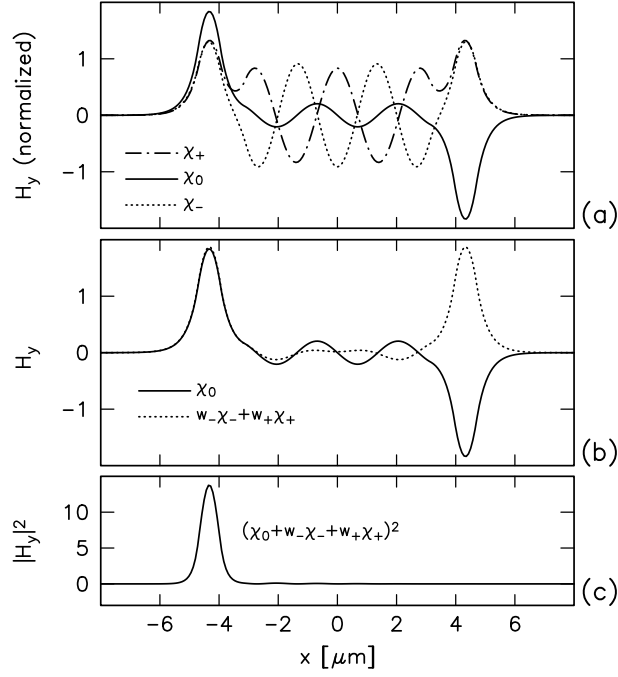


Figure 3: (a) Mode functions  $\chi_-$ ,  $\chi_0$ ,  $\chi_+$  ( $TM_6$ ,  $TM_5$ ,  $TM_4$ ) for the structure with parameters as in Fig. 2 and  $H = 6.261\mu\text{m}$ . Corresponding propagation constants are  $\beta_- = 10.8660/\mu\text{m}$ ,  $\beta_0 = 10.8772/\mu\text{m}$ ,  $\beta_+ = 10.8864/\mu\text{m}$ . The linear combination of  $\chi_-$  and  $\chi_+$  with weights  $w_- = \sqrt{w_{1-}/w_{10}} = 0.671$  and  $w_+ = \sqrt{w_{1+}/w_{10}} = 0.754$  is similar to  $\chi_0$  in the outer waveguide regions, apart from the reversed symmetry (b). The mode function of one outer waveguide can be approximated by a superposition of all three modes (c).

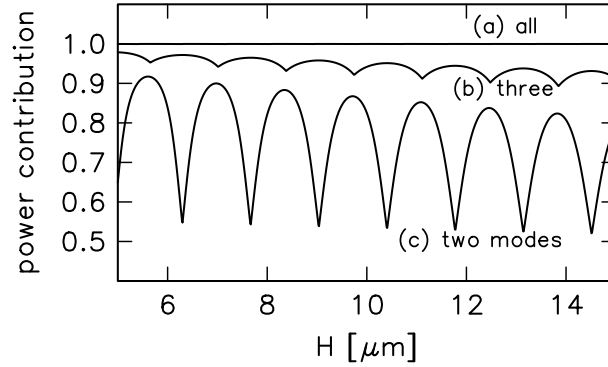


Figure 4: Contributions of different mode sets to the power transfer for zero device length versus the thickness of the central layer. (a): power transfer  $P_1(0)$  of the entire mode spectrum, (b): contribution  $\mathcal{P}_1(0)$  of the three most excited modes, (c): power transferred by the two most excited modes. In the neighbourhood of the maxima of curve (c) the coupling behaviour can be described approximately by the interference of two modes. Next to the maxima of curve (b) at least three modes have to be taken into account. We call these regions for  $H$  the two or three mode regime, respectively. Note that the power contribution of three modes in the three mode regime is larger than the contribution of two modes in the two mode regime.

Admittedly, the three mode approximation is somewhat crude. To obtain better results, more or all guided modes should be taken into account. However, for the purpose of finding promising points in a multidimensional parameter space, this 'three closest mode' approximation serves quite well, and we will elaborate it further.

Because of the symmetry of the entire structure and with the subsequent selection of propagation constants,  $\chi_0$  and  $\chi_-, \chi_+$  have opposite parities with respect to the mirror reflection  $x \rightarrow -x$ . Therefore, by choosing  $\phi_2(x) = \phi_1(-x)$ , the scalar products within the outer waveguide modes are related by  $\langle \phi_2, \chi_j \rangle = \pm \langle \phi_1, \chi_j \rangle$  for  $\chi_j(x) = \pm \chi_j(-x)$ . If the three modes are supposed to represent the outer waveguide modes exactly, i.e. if  $\mathcal{P}_1(0) = 1, \mathcal{P}_2(0) = 0$ , their mode weights satisfy the equations  $w_{10} + w_{1-} + w_{1+} = 1$  and  $w_{10} = w_{1-} + w_{1+}$ .

If  $\beta_0$  is closer to  $\beta_-$  than to  $\beta_+$ , define

$$\Delta\beta = \beta_0 - \beta_-, \quad \gamma = (\beta_+ - \beta_0 - \Delta\beta)/\Delta\beta, \quad r = w_{1-}/w_{10} \quad (3)$$

and

$$\Delta\beta = \beta_+ - \beta_0, \quad \gamma = (\beta_0 - \beta_- - \Delta\beta)/\Delta\beta, \quad r = w_{1+}/w_{10}$$

otherwise.  $\Delta\beta$  denotes the smallest difference between the propagation constants of neighbouring modes. It defines a characteristic coupling length  $L_c = \pi/\Delta\beta$ . Additionally one amplitude ratio  $r$  and the asymmetry parameter  $\gamma$  are sufficient to characterize the power contained in the input waveguide, as we shall see.

With the above definitions the power transfer function  $\mathcal{P}_1$  reads

$$\mathcal{P}_1(L) = \frac{1}{4} |1 + r \exp(i\pi L/L_c) + (1 - r) \exp(-i(1 + \gamma)\pi L/L_c)|^2. \quad (4)$$

Obviously, the conditions for the transmission to be complete —  $\mathcal{P}_1(L) = 1$  — are

$$L = 2mL_c \quad \text{and} \quad \gamma = j/m. \quad (5)$$

Likewise the transmission vanishes —  $\mathcal{P}_1(L) = 0$  — if

$$L = (2m + 1)L_c \quad \text{and} \quad \gamma = 2j/(2m + 1) \quad (6)$$

hold. In both cases  $m$  and  $j$  must be nonnegative integer numbers. Recall that (5) and (6) refer to the 'three closest modes' approximation. Parameters determined in this manner may serve as starting values for an optimization procedure which takes all modes into account.

The transferred power is minimal or maximal if the device length is an odd or even multiple of  $L_c$ , respectively. In contrast to the superposition of only two modes, the propagation constants must additionally satisfy the conditions (5) and (6) with  $\gamma$  as given by (3). Defining the usual coupling length  $L_c$  makes sense for three mode interference, even for nonequidistant propagation constants ( $\gamma \neq 0$ ).

The corresponding expressions for the two mode regime result for grossly unequally weighted modes  $\chi_-, \chi_+$ , i.e. for  $r \rightarrow 1$ . In this case the conditions (5) and (6) lose their significance, and maximum or minimum power transfer occurs at each multiple of the coupling length. This situation was investigated in Ref. [10].

Variation of the parameter  $H$  alters both  $L_c$  and  $\gamma$ . In Fig. 5 we have marked points  $(H, L_c)$  where the condition (5) for total power transfer is met. These points occur rather frequently, thus justifying the continuous curve  $L_c = L_c(H)$  for design considerations.

### 3 Magneto optic layers

We will now assume that one or more layers have a linear magneto optic effect. If the static magnetization is adjusted in the film plane and points perpendicular to the direction of propagation (transverse configuration, [14, 15]), the corresponding dielectric tensor  $\epsilon$  is

$$\epsilon = \begin{pmatrix} n^2 & 0 & -i\xi \\ 0 & n^2 & 0 \\ i\xi & 0 & n^2 \end{pmatrix}. \quad (7)$$

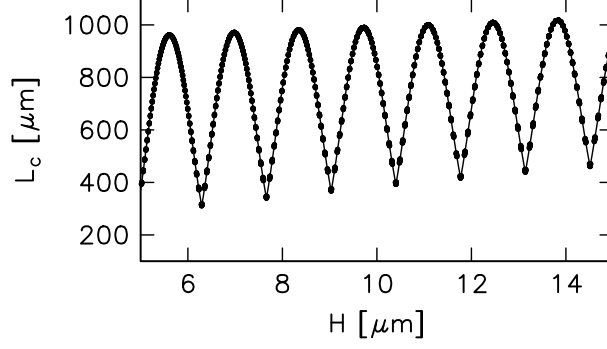


Figure 5: Coupling length  $L_c$  for different thicknesses  $H$  of the central layer. Parameters are as in Fig. 2. The line represents  $L_c$  according to (3). Regions for  $H$  with  $\mathcal{P}_1(2L_c(H)) = 1$  according to the three mode approximation are marked. At such points (5) holds approximately with  $m = 1$ , i.e.  $m\gamma(H)$  deviates from the next natural number by less than 0.1.

The off-diagonal elements are related to the specific Faraday constant  $\theta_F$  by  $\xi = n\lambda\theta_F/\pi$ . Scalar equations for TE and TM polarized modes may be derived just as for isotropic media. In first order,  $\xi$  does not affect the propagation of TE polarized light, so our further analysis concentrates on TM modes.

It is well known that the time reversal transformation  $(t, \mathbf{x}) \rightarrow (-t, \mathbf{x})$ ,  $\rho \rightarrow \rho$ ,  $\mathbf{j} \rightarrow -\mathbf{j}$ ,  $\mathbf{E} \rightarrow \mathbf{E}$ ,  $\mathbf{B} \rightarrow -\mathbf{B}$  is a symmetry of Maxwell's equations (using common notation). A wave propagating in the forward direction becomes a backward travelling wave with otherwise identical properties (reciprocity theorem). In a medium with linear magneto-optic effect, the static magnetization must change sign as well for the reciprocity theorem to hold. Since this is not the case, magneto-optic devices may exhibit nonreciprocal effects.

Our structure is mirror symmetric with respect to the  $x = 0$  plane. Its transmission properties can be studied by coupling light into the first waveguide only. Likewise, reversing the sign of the imaginary nondiagonal permittivity entry  $i\xi$  in all magneto-optic layers simulates reversal of the direction of propagation.

The waveguides may be investigated as multilayer structures with gyrotropic layers. Mode propagation constants and fields differ for opposite directions of propagation. These differences may be calculated by subtracting solutions for opposite  $\xi$  or by perturbation theory [16], resulting in the following expression.

Suppose the structure consists of  $N + 2$  homogeneous magneto-optic layers. Then the propagation constant  $\beta$  related to the mode  $\chi$  in the isotropic structure ( $\xi = 0$ ) changes to  $\beta + \delta\beta$ :

$$\delta\beta = \frac{1}{2} \sum_{j=0}^N \left( \frac{\xi_{j+1}}{n_{j+1}^4} - \frac{\xi_j}{n_j^4} \right) |\chi(h_j)|^2. \quad (8)$$

$h_j$  denotes the boundaries of the piecewise constant permittivity profile:

$$(n, \xi)(x) = \begin{cases} (n_0, \xi_0) & \text{if } x < h_0 \\ (n_j, \xi_j) & \text{if } h_j < x < h_{j+1} \\ (n_{N+1}, \xi_{N+1}) & \text{if } h_N < x \end{cases}. \quad (9)$$

If the layers of radiatively coupled waveguides are made of magneto-optic material, usually the coupling lengths  $L_c^f = \pi/\Delta\beta_f$  for forward and  $L_c^b = \pi/\Delta\beta_b$  for backward light propagation will be different. An isolator results if the device length  $L_{is}$  can be adjusted such that  $L_{is} = lL_c^f = (l \pm 1)L_c^b$  holds for a positive integer number  $l$ ,

$$L_{is} = \frac{\pi}{|\Delta\beta_f - \Delta\beta_b|}. \quad (10)$$

If  $l$  is even and light is injected at port A, it will leave the device at port B (see Fig. 1); if light is injected at port B, it will leave the device at port D. Likewise, if  $l$  is odd and light is injected at port A, it will leave the device at port C; if injected at C, it will leave at D.

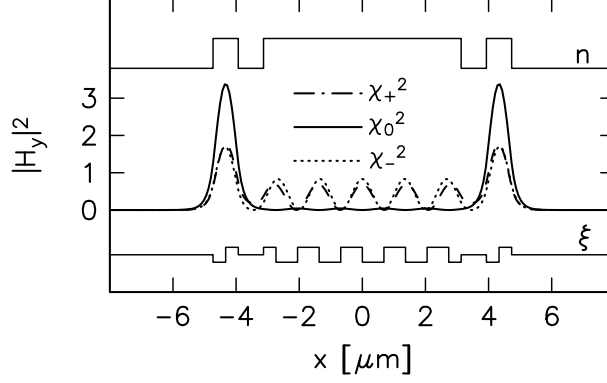


Figure 6: Absolute field values of the modes from Fig. 3. The refractive index profile is sketched above. The profile of the Faraday rotation shown below is adjusted to the shape of the mode functions to obtain optimal nonreciprocal phase shifts.

(10) defines the dependence of  $L_{is}$  on the tuning parameter  $H$ . Note that  $L_{is}$  is the length of an isolator only if  $L_{is}(H)/L_c^f(H)$  turns out to be an integer. Moreover, the conditions (5) and (6) with multiplicities  $l$  and  $l \pm 1$ , respectively, must hold for both  $L_c^f$  and  $L_c^b$ , at least approximately. Note that (10) is unnecessarily rigid because complete power transfer is required only in forward direction.

Using the notation of section 2, (10) may be rewritten as

$$L_{is} = \frac{\pi}{2|\delta\beta_{\pm} - \delta\beta_0|}. \quad (11)$$

To realize a short device, a large difference between the nonreciprocal phase shift of the two most relevant modes is required. At points  $x$  with maximum difference in the absolute values of the mode fields, boundaries between regions with different Faraday rotation must be inserted (see (8)). The modes  $\chi_0$  and  $\chi_+$  or  $\chi_-$ , respectively, show opposite symmetry with respect to  $x = 0$ . In the central layer their absolute field values are periodic in  $x$  with a period of  $2d \approx \pi/\sqrt{k^2 n_3^2 - \beta_*^2}$ . Therefore  $\xi$  should jump at  $x = \pm jd$ , with  $j = 1, 2, \dots$ ,  $|x| < H/2$ .

If the coupling region is made of layers of thickness  $d$  with alternating Faraday rotation, the nonreciprocal phase shift  $\delta\beta_0$  and  $\delta\beta_+$  or  $\delta\beta_-$ , respectively, have a different sign.  $L_{is}$  can be further reduced if the outer waveguides are built from double magneto-optic layers as well. In this case the two layers must be ordered properly to enhance the nonreciprocal phase shift caused by the magnetic grating in the central layer. These concepts are illustrated in Fig. 6.

## 4 Numerical Results and Examples

The following discussion assumes two different media. A nonmagnetic medium with smaller refractive index  $n_0 = n_2$  is used for the cladding and gap layers. The guiding regions are made of magneto-optic material (refractive index  $n_1 = n_3$ ) which can be properly doped to exhibit positive and negative Faraday rotation of equal magnitude (nondiagonal elements  $\pm i\xi$ ). These assumptions are realistic, see Ref. [3].

Fig. 7 compares potential device lengths of isolators based on radiatively coupled waveguides with identical refractive index profile. The values are estimated with the aid of (11).

If the outer waveguides are made of two layers, the total length can be shortened by a factor of 10 as compared to magneto-optic single layer outer waveguides provided that  $H$  is chosen within the three mode regime. In the case of only two relevant modes, both propagation constants are shifted in the same way because of approximately equally large amplitudes in the outer waveguides. This is the reason for the poles in curve 2 of Fig. 7. Such large variations vanish if the coupling layer is a magnetic grating. In the three mode regime, the device is half as long as compared to the double layer structures. It is further diminished by a factor of 3/4

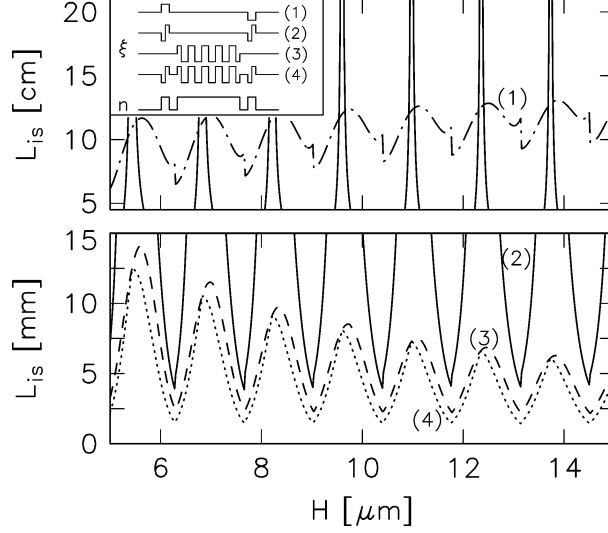


Figure 7: Isolator device length  $L_{is}$  versus the thickness  $H$  of the coupling layer. Different parts of the multilayer structures have been modeled to be magnetooptic: (1 – dash-dotted line) only the outer waveguides: single layers with opposite faraday rotation on both sides, (2 – continuous line) the outer waveguides: double layers of equal thickness with opposite Faraday rotation, (3 – dashed line) the central region: magnetic grating with alternating Faraday rotation, (4 – dotted line) the outer waveguides: double layers, additionally alternating Faraday rotation in the coupling layer. Parameters are as in Fig. 2,  $|\xi| = 0.005$ . Example profiles of Faraday rotation and refractive index for  $H = 6.261 \mu\text{m}$  are sketched in the inset.

if both the central region and the outer waveguides consist of magnetooptic layers. The following paragraphs refer to such structures.

The available material ( $n_0 = n_2, n_1 = n_3, \xi$ ), the light wavelength  $\lambda$  and the height  $h$  of the outer waveguides are assumed to be fixed, the gap width  $t$  and the coupler thickness  $H$  have to be optimized. We observed the following tendencies:

If  $t$  decreases, the modes of the outer waveguides deviate more and more from the modes of the entire structure which leads to larger coupling losses at input and output. If  $t$  increases, the coupling length increases in both regimes. In the three mode regime the minimal isolator length depends but weakly on  $t$  while gradients in  $L_{is}(H)$  increase for larger  $t$ . We are looking for values  $H$  for which  $L_c^f(H)$ ,  $L_c^b(H)$ , and  $L_{is}(H)$  simultaneously have their proper meaning as coupling or isolator length. Such values occur less frequently with increasing gap width  $t$ .

For given gap width  $t$ , regions with promising thicknesses  $H$  can be selected from charts like Fig. 7. In these regions points  $H$  must be searched which guarantee a proper isolation at a device length  $L$  close to  $L_{is}(H)$ . These simulations must consider all guided modes of the coupler structure to give reliable results.

Larger  $H$  improves the separation of the input and output waveguides, but the number of magnetic layers, hence the structuring effort, increases. The relevant propagation constants are more closely spaced, therefore coupling lengths increase and tolerance requirements for  $L$  and  $H$  become less strict. Also, additional modes contribute to the coupling process which results in larger transmission loss due to multimode interference.

Table 1 presents three example parameter sets which correspond to well performing isolator devices. We have calculated the interference of *all* guided modes, indicated by the symbol  $P$  instead of  $\mathcal{P}$  which stands for the 'three closest mode' approximation. The isolation is defined by  $10 \log P_1^f / P_1^b$ , the (forward transmission) loss by  $-10 \log P_1^f$ . Reflections at power input and output and the losses due to material absorption are neglected. The tolerance  $\Delta X$  of a length parameter  $X$  is declared as follows. If all other parameters remain fixed, then  $[X - \Delta X, X + \Delta X]$  is an interval of values such that isolation better than 20 dB and forward transmission loss below 0.5 dB are guaranteed. The parameters  $h$  and  $t$  have been varied for one of the outer waveguides only. The coupling region of structures (i), (ii), and (iii) is made up of 10, 16, and 28 layers of



	(i)	(ii)	(iii)
coupling layer thickness $H$ [ $\mu\text{m}$ ]	6.261	10.352	18.719
device length $L$ [ $\mu\text{m}$ ]	1512	1558	1504
isolation [dB]	38	55	38
forward transmission loss [db]	0.15	0.15	0.27
coupling layer tolerance $\Delta H$ [nm]	5	7	12
device length tolerance $\Delta L$ [ $\mu\text{m}$ ]	35	40	35
gap thickness tolerance $\Delta t$ [nm]	16	16	20
waveguide thickness tolerance $\Delta h$ [nm]	3	3	3

Table 1: Example parameters and tolerances for isolators based on planar radiatively coupled waveguides. The remaining parameters are  $\lambda = 1.3\mu\text{m}$ ,  $h = 0.8\mu\text{m}$ ,  $t = 0.8\mu\text{m}$ ,  $n_0 = n_2 = 2.18$ ,  $n_1 = n_3 = 2.30$ ,  $|\xi| = 0.005$ . See Fig. 1 for further explanations.

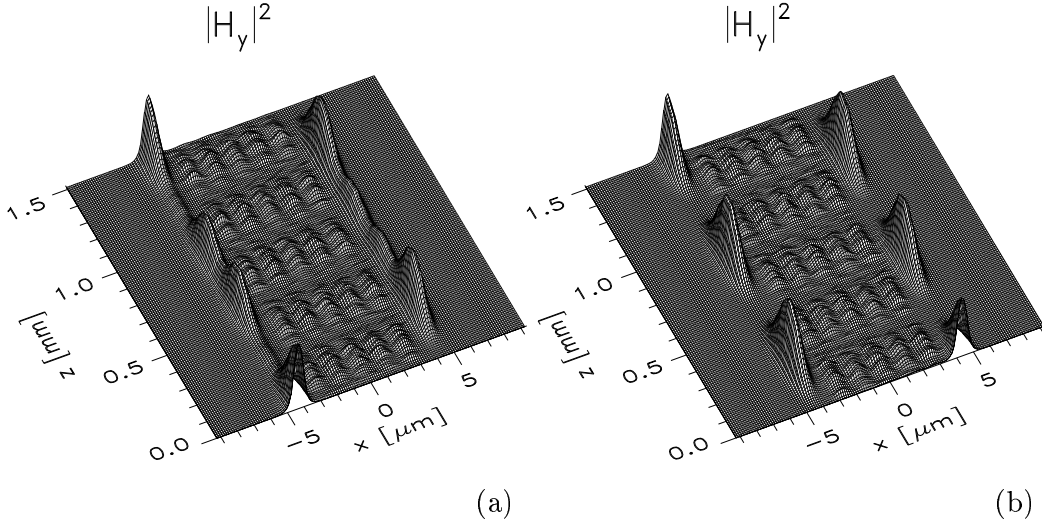


Figure 8: Light propagation in structure (i) of Tab. 1. The TM-polarized mode function of one outer waveguide is used as an initial field in  $z = 0$  (a) and  $z = 1.5\text{mm}$  (b). In the direction of transmission the power remains in the input waveguide (a), while in the opposite direction the power is guided to the other waveguide (b). Due to  $\gamma_b \approx 0$  an almost periodic interference pattern emerges in the backward direction (b).

alternating Faraday rotation. Fig. 8 illustrates light propagation in structure (i).

The three sample devices — which have been calculated and optimized with *all* guided modes — may be analyzed by the ‘three closest mode’ approximation as outlined in section 2. Conditions (10) and (5), (6) for good isolator performance are met, at least approximately, as demonstrated in Table 2. The ratios of device to coupling lengths should be integer numbers (4, 4, 2, 5, 3, and 3 in our case). Likewise, the asymmetry parameters  $\gamma$  turn out to be close to fractions of two small integers (1/2, 0, 1, 0, 2/3, and 0).

For comparison, a conventional nonreciprocal coupler (no central layer in Fig. 1) made from the same materials ( $n_0 = n_2$ ,  $n_1$ ,  $|\xi|$ ) with the same geometry of the coupled waveguides ( $\lambda$ ,  $h$ ) must be longer than 2.75 mm. This length results for a gap width  $t = 0$  and double layer waveguides. It is further enlarged by bends which are necessary for separating input and output ports. A gap width  $t = 0$  corresponds to a coupling length of 11.7  $\mu\text{m}$ , and a tolerance below 0.7  $\mu\text{m}$  for the total device length is required. The coupling region length increases to 10.5 mm for a gap of width  $2t = 0.8\mu\text{m}$ . Conventional coupler isolators are highly sensitive to alterations of the waveguide separation. The optimal value of 0.8  $\mu\text{m}$  must be maintained with a tolerance

	(i)	(ii)	(iii)
$L_c^f [\mu\text{m}]$	381	391	739
$L/L_c^f$	3.97	3.98	2.04
$\gamma^f$	0.504	0.012	1.015
$L_c^b [\mu\text{m}]$	309	507	522
$L/L_c^b$	4.89	3.07	2.88
$\gamma^b$	0.003	0.671	0.002

Table 2: Values characterizing the coupling behaviour for the structures of table 1. The values listed here are the subject of (5), (6) and (10) for good isolator performance according to the three mode approximation. See the text for further explanation.

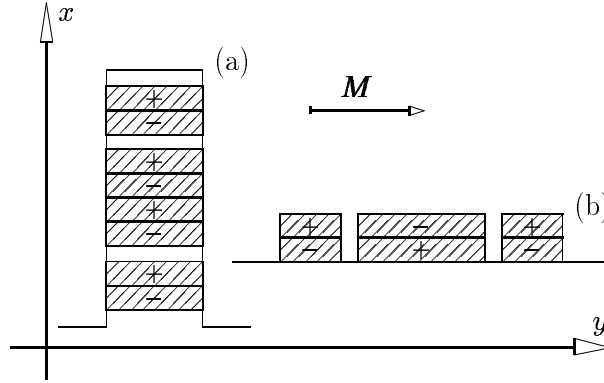


Figure 9: Concepts for isolator devices based on radiatively coupled waveguides. Cross sections perpendicular to the direction of propagation  $z$  are shown. Guiding magnetooptic layers are hatched, signs denote the signs of the Faraday rotation. Both concepts employ TM-polarized light ( $|H_y| \gg |H_x|$ ) and the magnetization points into the direction  $y$  parallel to the substrate surface.

better than  $\pm 0.4$  nm as can be estimated from the sinusoidal form of the power transfer and the dependence of the coupling length on  $t$ .

## 5 Rib waveguide concepts

Real integrated optical structures must guide the light in both transverse directions. Fig. 9 shows two possibilities how to exploit the advantages of radiatively coupled waveguides in three dimensions.

In (a) the multilayer structure proposed in section 3 is restricted laterally. The central strip and the second waveguide have been put onto the lower guide. To guarantee the required symmetry, the lower waveguide protrudes the substrate. In contrast to (a), structure (b) may be used as a circulator because the deviated light remains guided as well. (b) does not exploit the symmetry difference. The strongly different field amplitudes of the relevant mode functions in the coupling region and the outer waveguides cause nonreciprocal behaviour. Layers with opposite Faraday rotation would have to be realized side by side. However, it may turn out that isotropic outer waveguides in (b) allow sufficiently short devices as well.

## **6 Conclusions**

Radiatively coupled waveguides offer an attractive alternative to the conventional two waveguide coupler. Cross-talk between the optical channels is low since they are spatially well separated. Simple conditions for complete power transfer are obtained for both the two- and the three-mode regimes. An effective circulator can be designed if the central region consists of a stack of magneto-optic layers with alternating Faraday rotation. The manufacturing of such structures requires additional technological effort, but the expected significant improvement of performance characteristics with respect to the conventional nonreciprocal coupler would well pay off.

## **Acknowledgments**

We gratefully acknowledge financial support by Deutsche Forschungsgemeinschaft (Sonderforschungsbereich 225 and Graduiertenkolleg "Mikrostruktur oxidischer Kristalle").

## References

- [1] K. Ando. "Nonreciprocal devices for integrated optics". *Proceedings SPIE*, **1126**, 58–65, (1989).
- [2] H. Dötsch, P. Hertel, B. Lührmann, S. Sure, H. P. Winkler, and M. Ye. "Applications of Magnetic Garnet Films in Integrated Optics". *IEEE Transactions on Magnetics*, **28**(5), 2979–2984, (1992).
- [3] M. Wallenhorst, M. Niemöller, H. Dötsch, P. Hertel, R. Gerhardt, and B. Gather. "Enhancement of the nonreciprocal magneto-optic effect of TM modes using iron garnet double layers with opposite Faraday rotation". *Journal of Applied Physics*, **77**(7), 2902–2905, (1995).
- [4] T. Mizumoto, S. Mashimo, T. Ida, and Y. Naito. "In-plane magnetized rare earth iron garnet for a waveguide optical isolator employing nonreciprocal phase shift". *IEEE Transactions on Magnetics*, **29**, 3417–3419, (1993).
- [5] M. Levy, I. Ilic, R. Scarmozzino, R. M. Osgood, R. Wolfe, C. I. Guiterrez, and G. A. Prinz. "Thin-film-magnet magnetooptic waveguide isolator". *IEEE Photonics Technology Letters*, **5**, 198–200, (1994).
- [6] R. Wolfe, W.-K. Wang, D. J. DiGiovanni, and A. M. Vengsarkar. "All-fiber magneto-optic isolator based on the nonreciprocal phase shift in asymmetric fiber". *Optics Letters*, **20**, 1740–1742, (1995).
- [7] M. Shamonin, M. Lohmeyer, and P. Hertel. "Radiatively Coupled Magneto-Optic Waveguides". *Proceedings SPIE*, **2695**, 355–361, (1996).
- [8] A. Haus and C. G. Fonstad. "Three-Waveguide Couplers for Improved Sampling and Filtering". *IEEE Journal of Quantum Electronics*, **17**(12), 2321–2325, (1981).
- [9] S. M. Loktev, V. A. Sychugov, and B. A. Usievich. "Propagation of light in a system of two radiatively coupled waveguides". *Quantum Electronics*, **24**(5), 435–438, (1994).
- [10] M. Shamonin, M. Lohmeyer, and P. Hertel. "Directional coupler based on radiatively coupled waveguides". *Applied Optics*, (1996), submitted for publication.
- [11] J. P. Donnelly. "Limitations on Power Transfer Efficiency in Three-Guide Optical Couplers". *IEEE Journal of Quantum Electronics*, **22**(5), 610–616, (1986).
- [12] K. L. Chen and S. Wang. "The Crosstalk in Three-Waveguide Optical Directional Couplers". *IEEE Journal of Quantum Electronics*, **22**(7), 1039–1041, (1986).
- [13] J. P. Donnelly and H. A. Haus. "Symmetric Three-Guide Optical Coupler with Nonidentical Center and Outside Guides". *IEEE Journal of Quantum Electronics*, **23**(4), 401–406, (1987).
- [14] A. Erdmann, M. Shamonin, P. Hertel, and H. Dötsch. "Design of nonreciprocal couplers for integrated optics". *Proceedings SPIE*, **2150**, 183–192, (1994).
- [15] S. Yamamoto and T. Makimoto. "Circuit theory for a class of anisotropic and gyrotropic thin-film optical waveguides and design of non-reciprocal devices for integrated optics". *Journal of Applied Physics*, **45**, 882, (1974).
- [16] M. Shamonin and P. Hertel. "Analysis of nonreciprocal phase shifters for integrated optics by the Galerkin method". *Optical Engineering*, **34**(3), 849–852, (1995).